New Instruments and Methods of Measurement

THE INVESTIGATION OF DIFFUSION IN METAL OXIDES BY MEANS OF RADIOACTIVE TRACERS

N. S. GORBUNOV and V. I. IZVEKOV

Usp. Fiz. Nauk 72, 273-306 (October, 1960)

THE study of diffusion phenomena in the surface layers of metals, alloys, and some of their oxides, during oxidation and the deposition of diffusion coatings, is important in connection with the manufacture of many materials used in electronics, powder metallurgy, the silicate industry, airplane construction, etc.

The reaction between the surface of a metal (or alloy) and oxygen or some other oxidizing gas produces an oxide layer on the gas-solid interface. An understanding of the complicated mechanism involved requires knowledge of the structural properties of the oxide and of the diffusion parameters of the atoms, ions, and electrons participating in the reaction. The formation of oxides can greatly enhance or reduce the durability, heat resistance, service life, and other properties of manufactured articles.

In recent years the study of the structure of thin surface films has made considerable progress, and valuable experimental data have been collected and generalized.[1-3] A book written by Kubaschewski and Hopkins[4] deals with surface phenomena on metals and alloys. Original investigations[5] have been performed at the Institute of Physical Chemistry of the U.S.S.R. Academy of Sciences, but much work remains to be done on the production of high-quality protective coatings. Many theoretical questions have not been answered. No thorough study has been made of the kinetics and thermodynamics of the processes involved, and in many instances nothing is known about atom mobilities and the various quantitative characteristics of their motions. Wagner's theoretical laws[6,7] for the oxidation of metals and alloys have been confirmed experimentally only for a limited number of simple systems.

In the search for means of protecting metallic materials from premature breakdown it is important to determine the diffusion coefficients of the various components. Following the discovery of artificial radioactivity it has become possible to investigate diffusion in solids, and especially self-diffusion, on a broad scale. An isotope of gold was first used for this purpose.[8]

An expression for the temperature dependence of the diffusion coefficient,

$$D = D_0 \cdot \exp\left(-\frac{Q}{RT}\right), \qquad (1)$$

was obtained experimentally by Hevesy and Groh[9,10] in investigations of the self-diffusion of lead, and was also derived theoretically by Frenkel.[11] Experimental confirmation was obtained in many later investigations of diffusion in metals and oxides. At the same time, techniques employing radioactive tracers have been developed for the quantitative determination of diffusion parameters. These techniques, which are described in references 1 — 23, are now of basic importance in the pertinent physico-chemical experimentation.

During the past decade considerable data have been collected on diffusion in oxides of metals and refractories. The present article summarizes the relevant information.

EXPERIMENTAL TECHNIQUES

Samples for experimental investigations of diffusion in oxides have been prepared in different ways: out of oxide powders and their mixtures compressed into pellets, through the direct oxidation of a metal in an active gaseous medium, and out of natural and artificial single crystals. A radioactive tracer was deposited by vacuum condensation of a radioactive metal vapor, or by placing drops of a radioactive solution upon the surface of a sample. In the case of some electrically conductive oxides electrolysis has been used. The experimental diffusion process has been accelerated by high temperatures under different atmospheric conditions.

1. Experimental Apparatus

The apparatus must satisfy various requirements arising out of the necessity for controlling temperatures and atmospheric conditions, thus insuring the reliability of quantitative data on diffusion effects.

Reference 24 describes apparatus which controls the oxidizing potential of furnace gases in the production of iron oxides (wüstite, magnetite and hematite), and which is used for diffusion experiments in a H_2-H_2O (vapor) atmosphere. This apparatus consists of a gas-scrubbing train, a saturator (at constant temperature) for introducing definite amounts of water vapor into gases, and an electrically heated reaction vessel where the samples are suspended. The apparatus (Fig. 1) is made of glass or quartz and is operated at ~ 10 mm Hg. Argon was fed in for the purpose of cooling samples after diffusion experiments, which were controlled to within ± 1° C.

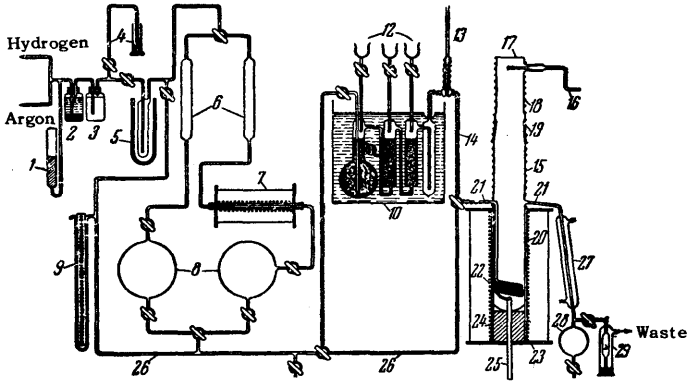

FIG. 1. Schematic diagram of the oxidation and diffusion unit. 1 – safety trap, 2 – vanadyl sulfate + Zn amalgam, 3 – gas scrubbing tower, 4 – vent line, 5 – cold trap, 6 – auxiliary drying towers, 7 – furnace containing Ti chips, 8 – vacuum-flask storage reservoirs, 9 – mercury manometer, 10 – constant-temperature oil bath, 11 – saturator, 12 – funnel tubes, 13 – mercury thermometer, 14 – electrically heated line, 15 – nichrome heating element, 16 – winch, 17 – optical window, 18 – glass head, 19 – ground joint, 20 – fused silica reaction chamber, 21 – graded silica-to-Pyrex seals, 22 – silica preheating spiral, 23 – kanthal-wound resistance furnace, 24 – alundum support, 25 – silica thermocouple well, 26 – bypass line, 27 – water-jacketed condenser, 28 – collecting flask, 29 – constant-head trap.

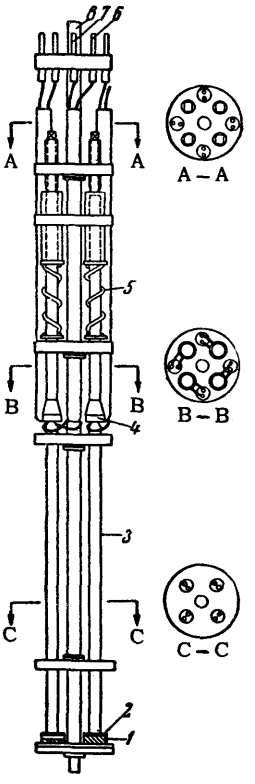

FIG. 2. Apparatus for diffusion experiments. 1 – samples, 2 – platinum plate, 3 – double-holed protection tube of quartz (for thermocouple), 4 – springs pressure on quartz tube, 5 – springs 6, 7, 8 – contacts for measuring emf of thermocouple and electrical conductivity.

In reference 25 Lindner has described apparatus (Fig. 2) for measuring diffusion coefficients, conductivity, and transport numbers in compressed and sintered pellets of oxide powders. Nonradioactive pellets were pressed against radioactive pellets, the contact being monitored by a sample of double thickness. In this way the electrical resistance of the clamped pellets was compared with a continuous pellet of thickness equal to the combined thicknesses, leading to a correction for imperfect contact. Following a diffusion anneal, when the redistribution of radioactivity between the radioactive and initially nonradioactive pellets was known, the diffusion coefficient was determined from the relationship

$$S = qc\sqrt{\frac{Dt}{\pi}}, \qquad (2)$$

where S is the radioactivity absorbed by the pellet, q is the contact area (cm^2), c is the concentration (counts/cm^2), D is the diffusion coefficient (cm^2/sec), and t is time (sec).

In order to obtain radioactive red PbO in connection with the investigation of powder reactions in silicate systems, the apparatus represented in Fig. 3 was used.[26] 15 ml of a 30% solution of lead nitrate (containing ThB) was heated in the reaction vessel to the boiling point, by means of a movable electric furnace (a tantalum coil between two Pyrex tubes), while very pure nitrogen was admitted. The addition of 30 ml of 50% potassium bicarbonate at first produced a whitish yellow precipitate, which gradually assumed red coloration. The preparation was then washed five times,

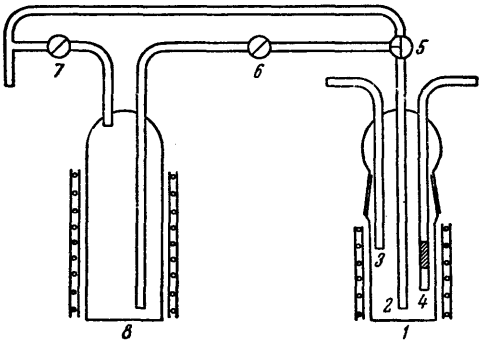

FIG. 3. Apparatus for the production of radioactive red PbO in the investigation of powder reactions in silicate systems. 1 – reaction vessel of high-quality glass, 2, 3 – glass tubes, 4 – glass frit, 5, 6, 7 – glass stopcocks, 8 – reserve vessel.

and was cooled in a nitrogen current after drying at 300° C.

For the investigation of Fe self-diffusion in FeO and that of Co in CoO under defined atmospheric conditions, Carter and Richardson[27] used the apparatus depicted in Fig. 4. For the work with FeO and with CoO above 1150° C the furnace had a platinum coil and 50-mm constant (to within ± 2° C) temperature zone at 1200° C. For CoO samples up to 1150° C a tantalum coil was used. The outside of the furnace was differentially lagged in order to provide a 100-mm constant-temperature zone. The reaction tubes were made of quartz glass; for high temperatures alumina and mullite tubes with Pyrex cone ends were employed. For the purpose of preventing vapor condensation in

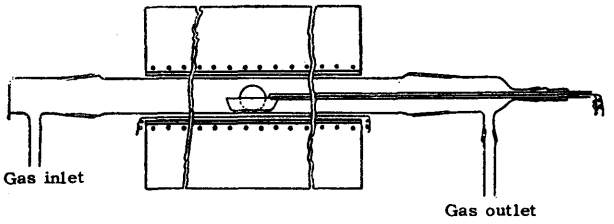

FIG. 4. Schematic diagram of furnace assembly.

the H_2-H_2O atmosphere a heating tape was wound around the cold parts of the apparatus. The entire assembly was tested for leaks.

For the purpose of studying Ca self-diffusion in calcium orthosilicate (Ca_2SiO_4) Lindner and Spicar[28] used a vacuum furnace (Fig. 5) having both geometric and thermal symmetry. The working part of the furnace was an alundum tube (60 mm long) surrounded by a heating element made of platinum wire (0.5 mm in diameter). The sample was placed in the middle of this tube, adjacent to a thermocouple junction. The furnace was equipped with a water jacket for cooling.

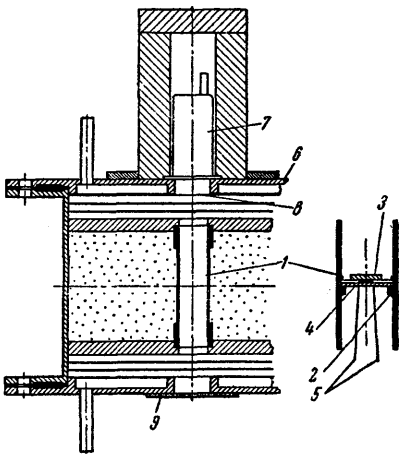

FIG. 5. Vacuum furnace. 1 – alundum tube (diameter 17 mm), 2 – circular flange of Al_2O_3, 3 – sample, 4 – two-hole disk (for thermocouple), 5 – platinum-platinum-rhodium thermocouple, 6 – surface of furnace, 7 – gas counter, 8 – dural foil, 9 – cemented quartz disk.

Radioactivity of the sample was measured continuously throughout the experiment by means of a gas counter mounted at one side of the alundum tube. The temperature of the diffusion anneal was raised to 1500° C without raising the temperature in the counter tube above 25 or 30° C. Diffusion coefficients in calcium orthosilicate were calculated with the aid of the activity records shown in Fig. 6.

Secco and Moore[29] used the apparatus sketched in Fig. 7 for investigating diffusion and exchange of Zn in ZnO crystals. A suspended quartz bucket contained 50 mg of radioactive ZnO crystals. The bottom of the reaction vessel held a weighed quantity of inactive Zn, which was sufficient to maintain the requisite pressure at the reaction temperature. Argon was added to maintain a pressure of 1 atm in order to prevent the evaporation of ZnO below this pressure. After evacuation to 5×10^{-5} mm at 200° C the vessel was sealed, and was then heated in a furnace that was controlled to within ±4° C. Zn vapor condensed on the inner

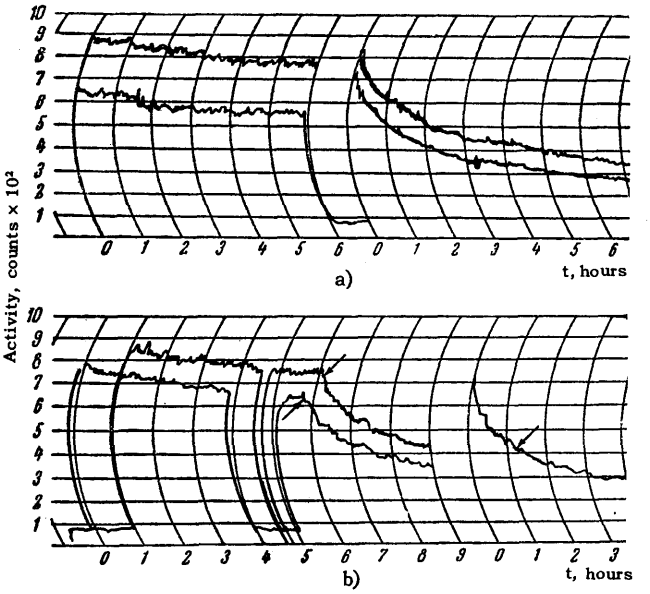

FIG. 6. Typical radioactivity records. a) at low and high temperatures; b) at left – in the crystallographic transformation region, at right – outside of this temperature region.

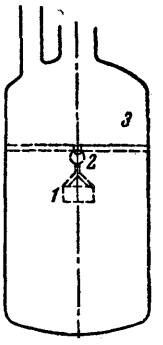

FIG. 7. Apparatus for investigating diffusion and exchange. 1 – quartz cup, 2 – cup suspension, 3 – exchange-reaction vessel.

walls, leaving the bucket practically free of adsorbed Zn. When the vessel had been cooled and opened, the bucket was removed and weighed to determine losses. The residual radioactivity of the ZnO crystals was then measured.

Lindner[30] used the apparatus represented in Fig. 8 to deposit a thin radioactive layer on oxide samples by means of vacuum condensation of radioactive vapor. The radioactive material was placed on a platinum foil that was raised to white heat by an electric current. When large currents were used the apparatus was water-cooled. The sample on which the radioactive tracer condensed was clamped to a metal block.

Fischer[31] used the apparatus represented in Figs. 9, 10, 11 and 12 to study diffusion processes between FeO and Al_2O_3 in strictly controlled gaseous atmospheres.

Our investigations of diffusion in oxides employed the apparatus that is partially described in references 32 and 33. The simplest version of the unit for diffusion anneals, which is represented in Fig. 13, consists

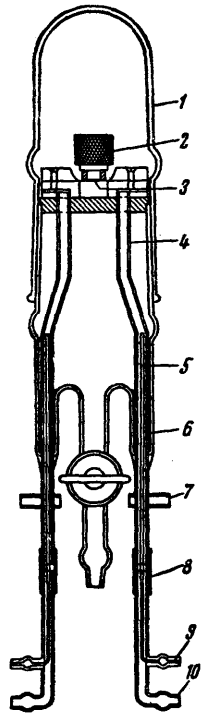

FIG. 8. Apparatus for depositing thin radioactive layers by means of vacuum evaporation and condensation. 1 – glass hood, 2 – metal block, 3 – radioactive substance, 4 – copper tube, 5 – water tube, 6 – Picein cement, 7 – current lead, 8 – rubber tube, 9 – water inlet, 10 – water outlet.

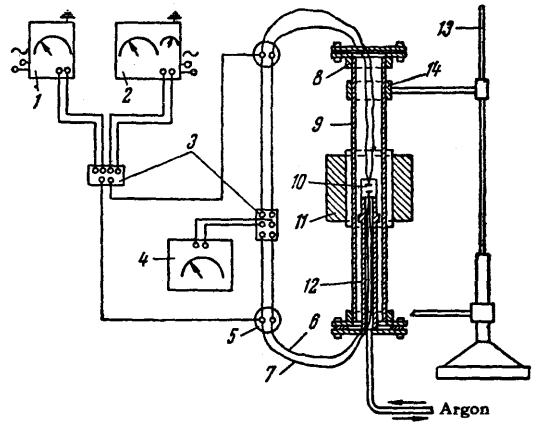

FIG. 9. Diagram of experimental setup. 1 – meter, 2 – vacuum tube voltmeter, 3 – switch, 4 – millivoltmeter, 5 – cold thermojunction, 6 – Pt-Rh wire, 7 – Pt wire, 8 – iron flange, 9 – sillimanite tube, 10 – measured body, 11 – Tamman furnace, 12 – supporting tube, 13 – stand, 14 – fastening.

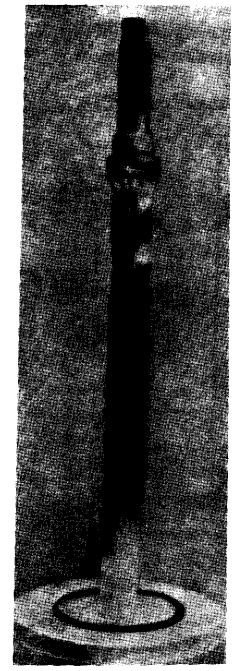

FIG. 10. Rubber fastening of measuring cylinder to sillimanite tube and supporting surface of iron flange.

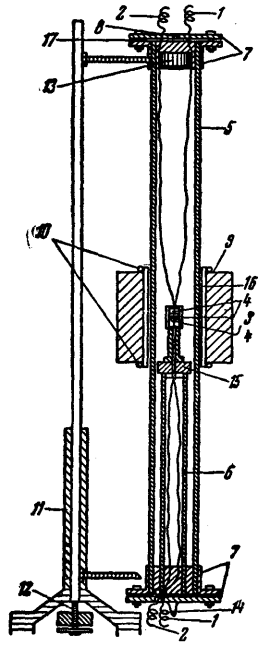

FIG. 11. Diagram of measuring tube with stand. 1 – Pt wire, 2 – Pt-Rh wire, 3 – measuring cylinder, 4 – Pt electrodes, 5 – sillimanite tube, 6 – supporting tube, 7 – iron flanges, 8 – viewing window, 9 – Tamman furnace, 10 – water cooling, 11 – stand, 12 – screw, 13 – fastening to stand, 14 – pump connection, 15 – hollow corundum body, 16 – carbon tube, 17 – rubber gasket.

of a ferroresonant stabilizer, an autotransformer and an electric furnace containing a quartz tube with two ground joints, one serving for the insertion of a thermocouple and the other for connecting with the vacuum pump system and the creation of prescribed gaseous atmospheres during anneals. The combined apparatus that we assembled consisted of four parts: a unit for deposition of radioactive coatings by means of vacuum evaporation, an electric furnace with a platinum resistance thermometer, a temperature-regulating circuit, and a quartz tube for inserting samples; these are shown in Fig. 14. Radioactive deposition was performed in a molybdenum glass vessel, within which sealed-in

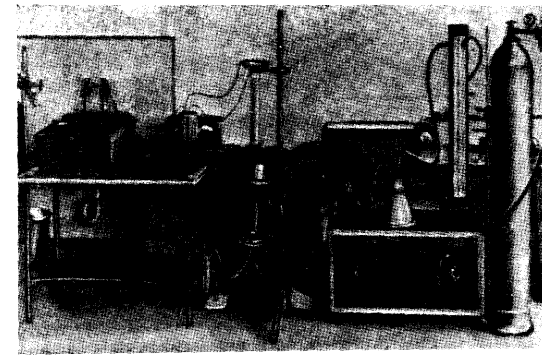

FIG. 12. Overall view of apparatus for electrochemical investigation of solid oxides at high temperatures.

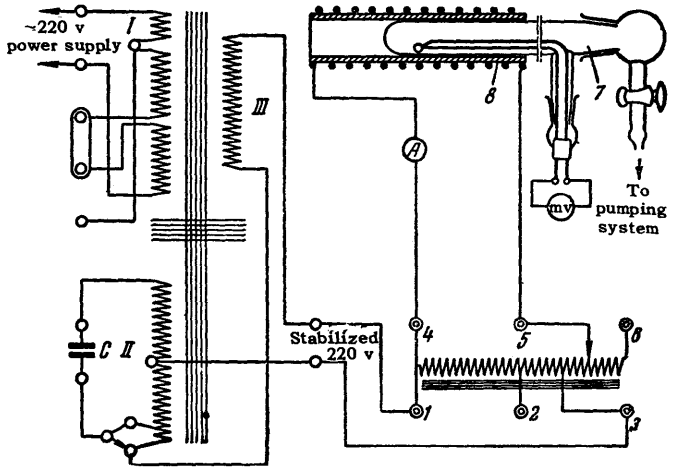

FIG. 13. Diffusion annealing unit with ferroresonant stabilizer. I, II, III – coils of ferroresonant stabilizer, 1–6 – autotransformer terminals, 7 – quartz tube, 8 – electric furnace.

molybdenum leads supported a coil and dismountable bulb containing the radioactive material, which after evaporation condensed on samples placed below it. The closed glass bulb served at the same time to limit the spreading of the radioactive vapor within the volume of the apparatus. In reference 34 a similar technique was used for coating samples with a tracer film. The regulating scheme, which we borrowed from reference 35, insured temperature constancy to within ± 0.5° C. In this circuit, increase of the furnace temperature changes the resistance of a platinum gauge in one of the bridge arms. The unbalanced bridge voltage is fed through an ac amplifier and phase-selecting stage to a detector. The rectified voltage is in turn amplified by a dc amplifier controlling a magnetic power amplifier that supplies current to the furnace coil. When the temperature falls below the prescribed level, thus unbalancing the bridge, the furnace-coil current reaches a maximum level, which is reduced as the proper temperature is approached. After the quartz tube had been loaded the electric furnace, with its operating mode already established, was lifted by counterweights, and the samples were heated to the requisite temperature within 1 or 2 minutes.

2. Methods for Determining Diffusion Coefficients in Metals and Metal Oxides

The diffusion coefficients must be known before reaction rates can be calculated. In most cases one determines the temperature dependence of the diffusion coefficient as given by Eq. (1). The activation energy Q of the diffusion process is usually associated with the lattice energy,[11,36] and D_0 is associated with the number of lattice defects.[37] The investigation of self-diffusion in solids was limited before the discovery of artificial radioactivity, and the experimental techniques in most instances did not satisfy the necessary requirements. Techniques for determining self-diffusion have been developed with and without the use of radioactive tracers.[38] These are partially reviewed in reference 12. The determination of D without the use of tagged atoms is less precise.

Nonradioactive methods for determining D include the following:

1) The use of tracers[39,40] which are chemically simi-

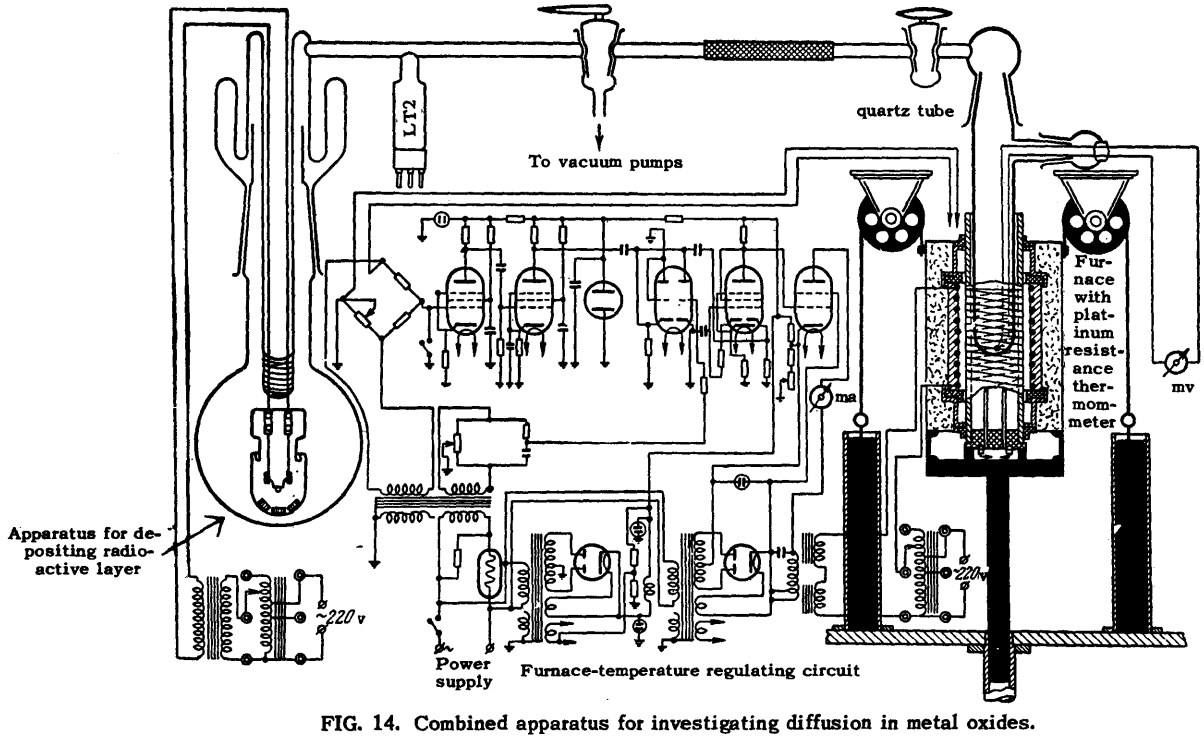

FIG. 14. Combined apparatus for investigating diffusion in metal oxides.

lar to the investigated substance. For example, CuI is used as a tracer for AgI. The mobility of the tracer in an AgI-CuI mixture is determined, after which the diffusion coefficient of Ag in AgI is calculated.

2) D is determined from ion conductivity[41] on the basis of

$$D = \frac{n\chi}{Fcze} kT, \tag{3}$$

where D is the diffusion constant, n is the transport number, χ is the conductivity ($ohm^{-1}\ cm^{-1}$), k is the Boltzmann constant, T is absolute temperature, c is the concentration (equivalents/cm^3), Z is the valence of the observed ion, F is the Faraday constant, and e is the electron charge.

3) Determination of D from the isotope exchange rate.[42]

4) Determination of D on the basis of phase transformations in the diffusion region.[43,44]

The most widely used among the radioactive methods are (see also reference 12):

5) The method of Stefan and Kawalki. Inactive pellets are pressed against an active pellet of measured thickness; the pellets are separated after the diffusion experiment. D is determined from the activity distribution in the initially inactive pellets.

6) Expansion of a thin radioactive film deposited on the sample. Following the experimental run the sample is sectioned into as many thin fractions as possible perpendicular to the diffusion direction. The radioactive concentration of each fraction is then measured, assuming

$$c = \frac{1}{\sqrt{\pi Dt}} \exp\left(-\frac{x^2}{4Dt}\right), \tag{4}$$

where c is the concentration in a layer at distance x from the surface of the sample, t is the diffusion-anneal time, and D is the diffusion coefficient. The function $\ln c = f(x^2)$ is a straight line of slope 1/4Dt. Banks[45] used this technique to measure self-diffusion coefficients of zinc ranging from 10^{-8} to 10^{-9} cm^2/sec.

7) The contact method. A perfect contact is established between an active pellet and an inactive pellet against which it is pressed; these are then inserted into a furnace. The contact is monitored by conductivity measurements. Equation (2) describes the diffusion of radioactive material; D is easily determined since the contact surface q and the initial concentration c are known. This technique is unsuitable for large values of D because recrystallization at high temperatures makes it difficult to section the pellets. This procedure has been used to determine diffusion coefficients from 10^{-12} to 10^{-15} cm^2/sec in various lead salts.

8) Alpha-particle absorption under the same initial conditions as for method 6). Ionization induced by a radiation beam emitted perpendicularly to the surface of the sample is measured before and after diffusion.[46] The value before diffusion is set equal to unity. Alpha particles enter an electroscope. The expression used for the concentration is

$$\int_0^{a-b} \frac{1}{\sqrt{\pi Dt}} e^{-\frac{x^2}{4Dt}} dx, \tag{5}$$

where a is the alpha-particle path in the investigated medium, and b is their path in air (and possibly in foil covering the electroscope), converted to the equivalent path within the sample. Since an electroscope measures both alpha radiation and the induced ionization current, the expression to be used for measuring the activity becomes complicated:

$$A = \int_0^{a-b} \frac{1}{\sqrt{\pi Dt}} (1 - \varphi(x))\, e^{-\frac{x^2}{4Dt}} dx, \tag{6}$$

where $\varphi(x)$ takes the ionization attenuation into account. D is calculated graphically. Details are given in references 46 and 47.

9) Absorption of radiation by recoil-atom emission. An electrically charged plate, at which the emission of recoil atoms is directed, is placed over the sample. Activity from the surface of the sample is represented by

$$A = \int_0^a \frac{1}{\sqrt{\pi Dt}} \left(1 - \frac{x}{a}\right) \exp\left(-\frac{x^2}{4Dt}\right) dx, \tag{7}$$

where t is time (sec), x is the distance of the recoil atom from the surface (cm), a is the path of the recoil atom in the investigated substance. D is determined from this equation with the aid of the curve in Fig. 15. In reference 46 this procedure was used to measure D from 10^{-14} to 10^{-17} cm^2/sec.

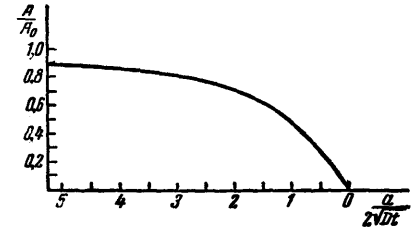

FIG. 15. Curve for determining diffusion constants by the recoil-atom method from variation of the relative activity A/A_0, for known experimental time t and recoil-atom path a.

10) Method of the active part of a pellet. An active layer is pressed upon an inactive pellet (the former comprising 0.5 or 0.25 of the total pellet thickness), and activity following the diffusion process is determined on both sides.

11) Active thin-layer method, based on the attenuation of surface beta activity. Using the relationship for concentration as a function of depth x in the layer,

$$c = \frac{Q}{\sqrt{\pi Dt}} e^{-\frac{x^2}{4Dt}}, \tag{8}$$

where Q is the total activity of the deposited layer, and the equation for absorption

$$A = \int_0^\infty ce^{-\mu x} dx, \tag{9}$$

where μ is the absorption coefficient, we obtain for the measured activity

$$A = A_0 e^{\mu^2 Dt} [1 - \psi(\mu\sqrt{Dt})] \quad (10)$$

which, for the determination of D, is solved by means of the curve of $A/A_0 = \psi(\mu\sqrt{Dt})$ (Fig. 16). This method[53] has been used to measure diffusion coefficients of Zn in ZnO from 10^{-8} to 10^{-11} cm^2/sec. The ranges of applicability of the different methods are shown in Fig. 17.

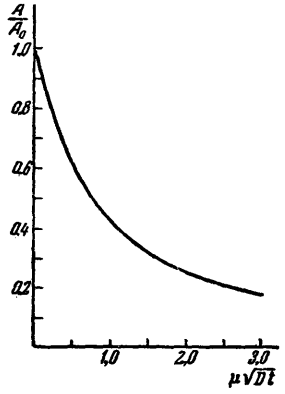

FIG. 16. Curve for determining diffusion constants by the active thin-layer method from variation of the relative activity A/A_0, for known experimental time t and absorption coefficient μ.

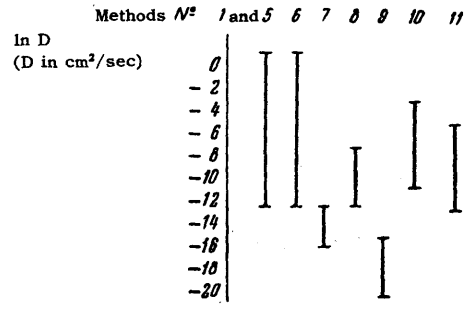

FIG. 17. Ranges of applicability of the various methods for determining diffusion coefficients in solids.

We shall now discuss the radioactive methods for determining diffusion coefficients in solids which have been developed by P. L. Gruzin, A. A. Zhukhovitskiĭ, and others. Gruzin[14] used 5×8×25 mm cobalt plates on which a radioactive film (1 to 5 microns) of Co^{60} was deposited electrolytically. The self-diffusion coefficient of Co was determined by removing successive layers, and computing their specific activity from the difference between the integrated activity of the sample measured before and after removal of each layer. For these samples, taking into consideration the initial and boundary conditions of the experiment, the solution of the diffusion equation is

$$c(x, t) = \frac{c_0 a}{\sqrt{\pi Dt}} \exp\left(-\frac{x^2}{4Dt}\right), \quad (11)$$

where c(x, t) is the concentration of the diffusing element at depth x from the surface of the sample, c_0 is the concentration of the element for an initial layer of thickness a, and t is the diffusion time. Replacing concentration in (11) by the activity i(x, t) of the diffusing atoms, we have

$$i(x, t) = \frac{\text{const}}{\sqrt{\pi Dt}} \exp\left(-\frac{x^2}{4Dt}\right). \quad (12)$$

Under these conditions the activity I_n of the sample after removal of a layer of thickness x_n is given by

$$I_n = \int_{x_n}^{\infty} i(x, t) \exp[-\mu(x - x_n)]\, dx, \quad (13)$$

where μ is the linear absorption coefficient of radioactive emission from the material of the sample. Substituting for i(x, t) in (13) and transforming, we have

$$I_n = \text{const} \cdot \exp(\mu^2 Dt + \mu x_n)\left[1 - \frac{2}{\sqrt{\pi}} \int_0^{\frac{x_n}{2\sqrt{Dt}} + \mu\sqrt{Dt}} \exp(-z^2)\, dz\right]. \quad (14)$$

From this we obtain

$$\left(\mu I_n + \frac{\partial I_n}{\partial x_n}\right) = \frac{\text{const}}{\sqrt{\pi Dt}} \exp\left(-\frac{x_n^2}{4Dt}\right) \quad (15)$$

In logarithmic form this equation becomes

$$\ln\left(\mu I_n + \frac{\partial I_n}{\partial x_n}\right) = -\frac{1}{4Dt} x_n^2 + \text{const}. \quad (16)$$

Because of the smallness of μ for gamma rays (about 0.3 cm^{-1}), we can in this case neglect μI_n. Consequently,

$$\ln \frac{\partial I_n}{\partial x_n} = -\frac{1}{4Dt} x_n^2 + \text{const}. \quad (17)$$

Equation (17) shows that $\ln(\partial I_n/\partial x_n)$ is a linear function of x_n^2 with its slope α equal to 1/4Dt. Our final formula is thus

$$D = \frac{1}{4t \tan\alpha}. \quad (18)$$

Lyashchenko[15] has proposed that the ratio of integrated activities be taken instead of the difference, and has calculated diffusion coefficients with the aid of nomograms. Gruzin and Litvin[16] have employed an absorption technique, by means of which the diffusion coefficient was calculated from the change of the ratio of tracer beta and gamma radiations. In this case we have

$$\frac{I_\beta I_{0\gamma}}{I_\gamma I_{0\beta}} = \exp(\mu_\beta^2 Dt)\,(1 - \operatorname{erf}\mu_\beta\sqrt{Dt}), \quad (19)$$

where $I_{0\gamma,\beta}$ is the integrated gamma or beta activity before the diffusion anneal, $I_{\gamma,\beta}$ is the intensity of gamma or beta emission after a given annealing time, μ_β is the beta-ray absorption coefficient of the investigated material, and t is the experimental time.

Kryukov and Zhukhovitskiĭ[18] determined diffusion coefficients as follows. A radioactive layer was deposited on one side of a thin sample (30 to 100 microns). After diffusion at constant temperature the activities I_1 and I_2 on both sides of the sample were measured. The equation

$$\ln\frac{I_1 - I_2}{I_1 + I_2} = \ln K - \frac{\pi^2 D}{l^2} t, \quad (20)$$

in which K is a constant, l is the sample thickness, and t is the diffusion time, was used to calculate D.

Zhukhovitskiĭ and Geodakyan[19] have developed a method for determining diffusion coefficients in thick samples without employing the absorption coefficient μ.

The choice of the method to be used for investigating diffusion in a solid depends primarily on the radioactive tracer that is used, the material of the sample, and the order of magnitude of the diffusion coefficient. The accuracy of the values obtained for diffusion coefficients is 15 — 30%. The largest error in the measurement of D often results from poor stabilization and inaccurate measurement of the diffusion temperature. A large effect is also produced by nonparallel removal of layers. We believe that improvement in this direction can considerably reduce the errors of experimental diffusion constants. In addition, careful observation of the requirements governing the preparation of samples, introduction of the tracer etc. in accordance with the initial and limiting experimental conditions, make these the most highly perfected methods at the present time.

INVESTIGATIONS OF DIFFUSION OF ELEMENTS IN METAL OXIDES

The relevant data can be divided into two parts. We shall first discuss diffusion in simple oxides. For convenience, the sequence of the presentation will be governed by the groups of the periodic table to which the metals of the oxides belong. The second part of the review will be concerned with complex oxides and refractories.

1. Diffusion in Simple Oxides

For group I of the periodic table we have data relating to diffusion in Cu_2O. Moore and Selikson[48] used Cu^{64} ($\frac{1}{2}\tau$ = 12.8 hrs). Cu_2O was prepared by oxidizing strips of spectroscopically pure copper at 1000° C in a current of pure dry nitrogen (300 cm^3/min), with pure dry oxygen admitted from an electrolytic cell at the rate 0.004 cm^3/min. Pieces of copper measuring 25 × 7 × 0.9 mm were completely oxidized in 24 hours and exhibited the large-grained structure of Cu_2O (grain size ~ 1 mm). A 48-hour anneal followed the oxidation process. By dipping into an active solution of cupric nitrate a thin Cu^{64} layer was deposited on the samples, with one side and the edges protected by paraffin wax. The active faces were then placed in light contact, and were maintained for periods ranging from 10 min at 1000° C to 8 hours at 800° C in the same atmosphere that was used for their preparation. Following the diffusion anneal the back side of each sample was coated with Glyptal varnish for the purpose of mounting on a glass rod. Successive layers were then etched off in 50% HNO. Following each removal process, radioactive Cu^{64} was deposited on a polished and weighed copper disk, whose activity represented the activity of the removed layer. This procedure determined the depth dependence of radioactivity in the sample as a basis for computing the diffusion coefficient. The diffusion of Cu in Cu_2O at 800 — 1000° C yielded $D = 0.0436 \exp(-36{,}100/RT)$. Values of D obtained from diffusion measurements are in good agreement with calculations based on electrical conductivity and transport numbers. The same investigators also showed experimentally that the parabolic oxidation rate constant of copper is given by $k \cong 4D$. They suggested that cation diffusion in Cu_2O is a mechanism employing the relatively high concentration of vacancies. In references 49 — 52 the diffusion coefficients of P^{32}, Au^{198}, I^{31}, S^{35}, and Ag^{110} in cuprous oxide were determined. Cu_2O or Cu was dipped into a solution containing the tracer; following suitable annealing, the usual method was used to measure concentration as a function of depth. The diffusion coefficient of sulfur in Cu_2O was found to be independent of the initial concentration of diffusing impurity deposited on a sample. In polycrystalline Cu_2O admixtures usually penetrate to a greater depth. Electrical conductivity is of the same order of magnitude in both polycrystalline and monocrystalline Cu_2O, and is somewhat enhanced by an impurity. This effect is more pronounced in connection with Ag, less so with P, and is insignificant with S. The curve representing the temperature dependence of electrical conductivity exhibits a bend at low temperatures when Ag or S is introduced into Cu_2O. Table I gives the diffusion coefficients of some elements in Cu_2O. These investigations were performed in connection with the study of the semiconductor properties of Cu_2O.

TABLE I

Tracer	Temperature, °C	Diffusion coefficient, cm^2/sec
Au	1000	$1{,}03 \cdot 10^{-9}$
I	1020	$8 \cdot 10^{-9}$
	1000	$0{,}89 \cdot 10^{-8}$
P	1020	$2{,}1 \cdot 10^{-8}$

In connection with oxides of group-II elements we shall discuss diffusion in ZnO, CaO and BaO. Lindner[53] used a hand press to prepare pellets of ZnO powder with densities 4.6 — 5.5 g/cm^3, which were sintered in air at 1300° C. Zn^{65} was used as the tracer. In this investigation of the oxidation of metallic zinc D was determined by both the active thin-layer method and the contact method.[13] In the active thin-layer method a layer of radioactive metallic zinc (1 mg) was vacuum deposited on the face of a sample, which was then inserted into a furnace; the layer was oxidized to ZnO in 2 — 3 min at 800° C. D was determined through two continuous measurements of activity. In one case an 0.5-mm aluminum foil was superposed for the measurement of gamma radiation; in the absence of the foil the combined beta and gamma radi-

ation was measured. The difference between these two measurements represented the beta radiation, the attenuation of which through absorption, as diffusing radioactive atoms penetrated deeper, yielded D by means of the curve $A/A_0 = f(\mu\sqrt{Dt})$. Here A is the beta activity of the tracer after an anneal lasting t seconds, as measured on the side of the active layer, A_0 is the initial activity, and μ is the absorption coefficient (cm^{-1}). In this experiment D can also be found by determining concentration gradients of active materials through the removal of thin layers. The accuracy of the result is then greater because it is possible to obviate a correction for the evaporation of the radioactive substance during absorption measurements. The limits of applicability of the active thin-layer method for determining D were estimated to be $10^{-8} - 10^{-12}$ cm^2/sec. In the contact method D is determined through the passage of radioactive Zn^{65} from an active to an inactive sample of ZnO; such pairs of samples were pressed together in a holder. In this case the range for D is $10^{-12} - 10^{-16}$ cm^2/sec. Samples with a deposited radioactive layer of Zn^{65} were annealed in air within platinum boxes surrounded by platinum and platinum-rhodium coils. For the diffusion of Zn in ZnO at 800 — 1370° C the result was $D = 1.3 \exp(-73{,}700/RT)$. Both boundary and volume diffusion were included and could not be distinguished. The activation energy of Zn diffusion in ZnO differs considerably from the activation energy for the oxidizing of metallic Zn, which was determined for temperatures below 419° C.

Reference 29 contains a more detailed investigation of Zn oxidation. Here the diffusion and exchange of Zn with ZnO crystals were carefully studied by means of an exchange-reaction vessel (Fig. 7). Exchange between Zn vapor and ZnO crystals was measured between 900° and 1025° C. ZnO crystals containing radioactive Zn^{65} were prepared through a reaction between Zn vapor and atmospheric oxygen. Crystal samples were inserted into a small quartz bucket suspended in the reaction vessel, and were then weighed. After sufficient pure Zn had been added to produce the requisite vapor pressure, the vessel was evacuated and sealed. The ZnO sample contained about 1000 grains of 0.01-mm average diameter and was carefully graded with respect to diameter. At various times the bucket was withdrawn for measurements of the residual activity of ZnO. The exchange reaction was controlled, with the exception of the initial stages, by the diffusion of Zn in ZnO. At a Zn vapor pressure of 1 atm the result $D = 4.8 \exp(-73{,}000/RT)$ was obtained. The most likely exchange reaction appeared to be the displacement $*Zn^{+2} + Zn_i^{+} = Zn^{+2} + *Zn_i^{+}$ (where Zn_i^{+} is the singly dissociated interstitial Zn ion) which involves the diffusion mechanism. It is interesting that the diffusion coefficients obtained by Lindner for sintered ZnO samples differ very little from those for single crystals in the work that has just been described.

Roberts and Wheeler[54] state that up to 1300° C Zn diffuses in ZnO mainly along grain boundaries. By means of mechanical sectioning, the distribution of Zn^{65} in pressed and sintered samples (with density at least 93%, grains from 10 to 100 microns and purity above 99.9%) was determined in the range 800 — 1300° C after storage in oxygen or argon. The radioactive layer was ~1 micron thick. Radiographic investigation confirmed the predominance of Zn diffusion along oxide grains. For volume diffusion $D = 0.1 \exp(-89{,}000/RT)$; for boundary diffusion $D = 10^3 \pm 2 \exp[(-69{,}000 \pm 12{,}000)/RT]$.

For the ratio of the activation energies $Q_{bound}/Q_{vol.} = 0.77 \pm 0.13$ was obtained. It was also established that D can diminish with the increase of excess Zn in the oxide. This result is more easily brought into agreement with the usually assumed model of interstitial Zn in ZnO than with a model which allows only for anion and cation vacancies.

In reference 55 Lindner reported measurements of self-diffusion and of the transport number of Ca^{45} in CaO, which are important for investigations of the reaction mechanism in surface layers and of the activation of cathode oxidation.[56] Calcium carbonate was heated to 900° C and was then compressed into disks 10 mm in diameter and 1 — 2 mm thick; these were then maintained at 1450° C for about 10 hours. The average density was 3.1 g/cm^3, while the greatest density was 3.25 g/cm^3. The half-life of radioactive Ca^{45} is 152 days. The absorption coefficient μ was determined for beta rays in calcium glass ($\rho = 2.405$ g/cm^3) and in Al. For CaO pellets $\rho = 3.1$ g/cm^3 and $\mu = 430$ cm^{-1}. Diffusion coefficients were determined in three ways: from the active part of the sample, from a radioactive thin layer and by the contact method.[57,13,25] The active-part method can be used for determining D up to 10^{-10} cm^2/sec. Each of the pressed samples employed for this purpose consisted of active and inactive parts; the reduced radioactivity of the active part and its increase in the inactive part as a result of diffusion were observed. D can be calculated from the time dependence of the change of activity. The measurement of conductivity and of the transport number employed the sample holder used in the contact method,[53] with contact between the platinum electrodes and the pellets established through a 0.01-mm aluminum foil. For the determination of the transport number, an active and an inactive sample were pressed together in the holder (or three samples with the active one in the middle). The applied potential of ~1000 v induced a current of ~1 ma in CaO at the experimental temperatures. The active-part method and the radioactive thin-layer method were very inefficient for measuring the self-diffusion of Ca in CaO. In the first case, because of the excessive porosity of CaO the activity resulting from boundary diffusion quickly approached its limit, while in the second case the investigator was unable to vaporize CaO. Chemical deposition of the radioactive layer produced unsatisfactory contact between

this layer and the sample, and the value obtained for D was not reproducible. Positive results were obtained when the radioactive layer was deposited through transport in an electric field. Deposition was possible in this case with a transport number greater than 10^{-4}, excluding the disturbing factor of Joule heat generated by passage of the electric current. All measurements were performed in air. The contact method furnished the most precise results. The temperature dependence from 850° to 1600° C was found to be $D = 0.4 \times \times \exp(-81{,}000/RT)$. This characterized mainly the volume diffusion,[58] which is found by determining concentration gradients as layers are ground off. The diffusion coefficient resulting from ion conductivity was determined from (3). Results for D based on (3) are in good agreement with results obtained in ordinary diffusion experiments without electric fields. In the first instance the diffusion of calcium ions is, of course, somewhat enhanced.

The diffusion of Ba^{140} in BaO was investigated radiochemically by Redington.[59] Radioactive barium in the form of BaO was vacuum evaporated and condensed on a BaO crystal. The crystal was sectioned to determine both the diffusion rate and the relationship between the diffusion coefficients of charged and neutral particles at different temperatures. Two simultaneous diffusion mechanisms were noted at 1077 — 1227° C. One of these transports charges, while the other is characterized by the diffusion of neutral atoms having a diffusion coefficient which is 20 times greater than that of charged particles and which ranges from 10^{-11} to more than 10^{-8} cm^2/sec. In BaO crystals annealed at 327 — 1027° C only the diffusion of neutral barium atoms was detected, with diffusion coefficients ranging from 10^{-13} to 10^{-11} cm^2/sec.

Group III of the periodic table is represented by data on the diffusion of iron in aluminum oxide (corundum).[34,60,61,62] Al_2O_3 samples were prepared by compressing oxide powders, which were then vacuum (10^{-2} mmHg) sintered at the highest temperature reached in the diffusion experiments. Radioactive Fe^{59} was vacuum evaporated and condensed on oxide samples. Diffusion coefficients were measured by removing layers; in this way an attempt was made to distinguish grain-boundary and volume diffusion of iron in Al_2O_3. The absorption technique was ineffectual, because the diffusion coefficient of Fe in Al_2O_3 is relatively small. The results are shown in Table II.

Group IV is represented by investigations of diffusion in TiO_2 (rutile), SnO_2 and PbO. Diffusion of iron in rutile[61,62] was investigated both in air and in a vacuum by means of both the absorption and layer-removal techniques. Fe^{59} served as a tracer in pressed and sintered rutile samples. The experimental temperature range was 770 — 1000° C. Both volume and boundary diffusion were detected in 1 — 10 micron TiO_2 grains. The diffusion coefficients for vacuum-annealed samples were 1 or 2 orders of magnitude greater than those for air-annealed samples (Table II).

For the investigation of diffusion in tin oxide the authors of reference 63 used compressed samples that had been sintered at 1400 — 1450° C, with density 4 g/cm^3 and appreciable porosity. Tin isotopes with mass numbers 119, 121, 123 and 125 were employed in both the active thin-layer and contact methods. An active thin layer was deposited by vacuum evaporation. At 1000 — 1260° C, diffusion of tin in tin oxide is represented by $D = 10^6 \exp[(-118{,}700 \pm 3700)/RT]$.

Lindner[64] investigated the self-diffusion of Pb in sintered PbO pellets, using ThB (Pb^{212}) as the tracer. Diffusion experiments were performed either in a vacuum or in pure nitrogen by the contact method. Temperatures were maintained constant to within ± 2° C. The initial activity of the radioactive PbO layer was of the order 10^4 counts/min per milligram. The temperature dependence of D in the range 400 — 600° C, above and below the transition point (488° C) of $PbO_{red} \rightleftarrows PbO_{yellow}$, is represented by $D = 10^5 \times \times \exp(-66{,}000/RT)$. The error in the activation energy is estimated at ~ 10%, with a somewhat greater error for the coefficient D_0 of the exponential function. D includes a certain amount of grain-boundary diffusion, which occurs simultaneously with volume diffusion.

Lindner and Terem[65] also investigated Pb diffusion in PbO, preparing samples as follows. Disks of 8 mm diameter and 2 mm thickness made of analytically pure (99.999%) lead were cleaned and etched in 20% HNO_3 and were oxidized in an oxygen current at different temperatures, their weight increase being determined at definite time intervals. It was found that the PbO film, as in the cases of some other metals, was preserved intact above the melting point of lead (327° C). Increase of weight was accurately represented by a parabolic function of time. The diffusion constant of radioactive lead (ThB = Pb^{212}) was measured by the alpha-recoil method. Diffusion coefficients were calculated on the basis of curves for the relative level of radiation as a function of time at different temperatures. The experiments were in full agreement with data previously obtained by Lindner for sintered PbO.

In connection with group VI we find two reports of diffusion in Cr_2O_3. Lindner and Akerström[67] measured diffusion in sintered Cr_2O_3 powder compacts using the absorption and contact methods. The structure of the oxide samples was determined through x-ray analysis. This investigation is of interest in connection with the oxidation of chromium. For the diffusion of chromium in chromium oxide at 1000 — 1350° C the result was $D = 4 \times 10^3 \exp(-100{,}000/RT)$.

In reference 34 sintered Cr_2O_3 powders were also investigated, with the result $D = 4.29 \times 10^{-8} \times \times \exp(-22{,}000/RT)$ for Cr diffusion and $D = 4.95 \times 10^{-} \times \exp(-44{,}000/RT)$ for Fe dissusion in Cr_2O_3.

In connection with group VIII we find data on diffusion in iron oxides, NiO, and CoO.

Reference 24 reports extensive work on iron diffu-

sion in iron oxides. The investigated samples were artificial wüstite and magnetite, produced by direct oxidation and prolonged exposure to high temperatures for the purpose of homogenizing spectroscopically pure iron. The wüstite and magnetite were compact products. In the case of hematite a single natural crystal was used, since direct oxidation did not yield a suitable product for diffusion experiments. Spectroscopic examination of the original iron used to prepare wüstite and magnetite showed the following composition: oxygen — 0.02%, nitrogen — 0.001%, hydrogen — 0.005%, carbon — 0.005%, other impurities — 0.02%. The wüstite and magnetite samples were cylinders 2 mm in diameter and 1.5 — 2 mm thick. From the natural hematite crystals 18×13×6 mm parallepipeds were cut with the largest face perpendicular (or parallel) to a fundamental {001} face. Laue apparatus was used to determine the orientations of crystal faces. Radioactive Fe^{55} was obtained from iron chloride. Since the solution was a mixture of Fe^{55} ($\tau/2$ = 2.9 yrs) and Fe^{59} ($\tau/2$ = 46 days), storage for more than a year was required to reduce the concentration of Fe^{59} to less than 0.5%. Purification was effected through prolonged ether extraction, after which the residue was brought to the desired level of activity with distilled water. For the purposes of oxidation, homogenization, and diffusion annealing of samples in special apparatus, the following equilibrium oxidizing atmospheres were used: for FeO 20% H_2 and 80% water vapor; for Fe_3O_4 10% H_2 and 90% water vapor.

TABLE II. Diffusion data for simple oxides

No.	Diffusing substance	Oxide (diffusion medium)	Experimental temperature range, °C	Numerical coefficient of exponential, cm²/sec	Activation energy, cal/mole	Reference
1	Cu^{64}	Cu_2O	800—1000	0.0436	36100	48
2	Zn^{65}		800—1370	1.3	73700	53
			900—1025	4.8	73000	29
			800—1300	10^{-1}	89000	54
				in grain volume		
				$10^{3}\pm2$	69000±12000	
				along grain boundaries		
3	Ca	CaO	850—1600	0.4	81000	55
4	Fe^{59}	Al_2O_3 (corundum)	900—1100	$9.18\cdot10^{-8}$	27600	61, 62
				in grain volume		
				$1.37\cdot10^{-8}$	11000	
				along grain boundaries		
			900—1200	1.13	82000	34
5	Fe^{59}	TiO_2 (rutile)	800—1000 in air	$1.98\cdot10^{-2}$	55000	61, 62
				in grain volume		
				$1.10\cdot10^{-8}$	12600	
				along grain boundaries		
			770—1000 vacuum anneal	$1.92\cdot10^{-1}$	55400	
				in grain volume		
				$6.17\cdot10^{-6}$	13800	
				along grain boundaries		
6	Sn	SnO_2	1000—1260	10^{6}	118700±3700	63
7	Pb^{212}	PbO	400—600	10^{5}	66000	64, 65

TABLE II. (Continued)

No. п/п	Diffusing substance	Oxide (diffusion medium)	Experimental temperature range, °C	Numerical coefficient of exponential, cm^2/sec	Activation energy, cal/mole	Reference
8	Cr^{51}	Cr_2O_3	1000—1350	$4 \cdot 10^3$	100000	67
				$4.29 \cdot 10^{-8}$	22000	34
9	Fe^{59}	Cr_2O_3		$4.95 \cdot 10^{-6}$	44000	
10	Fe^{55}	FeO	700—1000	0.118	29700	24
		Fe_3O_4	750—1000	5.2	55000	
		Fe_2O_3	1000—1217	$4 \cdot 10^5$	112000	
11	Fe^{59}	Fe_3O_4	770—1200	$1.27 \cdot 10^{-3}$	36200	32, 61
				in grain volume		
				0,25	53900	
				along grain boundaries		
12	Fe^{59}	Fe_2O_3	750—1300	$4 \cdot 10^4$	112000	69
13	Fe^{55}	FeO	700—1000	0.014	30200	27
	Co^{60}	CoO	800—1350	$2.15 \cdot 10^{-3}$	34500	
14	Ni^{63}	NiO	1140—1400	$2.8 \cdot 10^5$	119500	67
15	Mixture of Ni^{59} and Ni^{63}	Polycrystalline NiO		$5 \cdot 10^{-4}$	44200±3000	71
		Monocrystalline NiO		$3.9 \cdot 10^{-4}$	44200±3000	

Diffusion annealing of hematite took place in an oxygen atmosphere at 1 atm. Radioactive Fe^{55} was deposited electrolytically from an aqueous $FeCl_3$ solution containing 4 mg of radioactive iron per milliliter. Electrolysis lasted 1 to 3 minutes at 0.1 amp/cm^2. The average thickness of the deposited layer was $\sim 10^{-5} - 10^{-6}$ cm, with the radioactivity level at 8000 — 12,000 counts/min. The diffusion annealing time was measured from the instant when the sample reached furnace temperature (90 sec after its insertion). Cooling (gas quenching) took place in dry nitrogen. The diffusion coefficient was determined from the diminution of beta radiation during diffusion. The absorption coefficient was calculated from

$$\mu = \varrho\,(90.9 f_{Fe} + 32.2 f_O), \qquad (21)$$

where ρ is the density of the oxide, and f_{Fe} and f_O are the respective fractions of iron and oxygen by weight.

It was noted that during the oxidation of iron samples a large concentration gradient is present since the interior is richer in iron than the surface layer. If this gradient is not eliminated by homogenization, the diffusion of iron ions within a disk can be slowed down and thus yield a low value of D. It is therefore recommended that homogenization take place at the highest possible temperature. The same investigation showed how the diffusion coefficient is affected by the composition of the sample (or the number of Fe vacancies per unit volume of the oxide, such as wüstite, calculated from the deviation from its stoichiometric composition of 77.73% Fe). The greatest effect was observed at the highest of the three experimental temperatures (983° C), when D in wüstite increases by a factor of almost four, as the percentage of Fe diminishes (or the number of vacancies increases), between the iron-rich and oxygen-rich boundaries of the stable wüstite region (Fig. 18).

With samples of determined stoichiometric composition the following temperature dependences were obtained: 1) for $Fe_{0.907}O$ (76.02% Fe) at 700 — 1000° C, $D = 0.118 \exp(-29{,}700/RT)$ (Fig. 19); 2) for $Fe_{2.993}O_4$

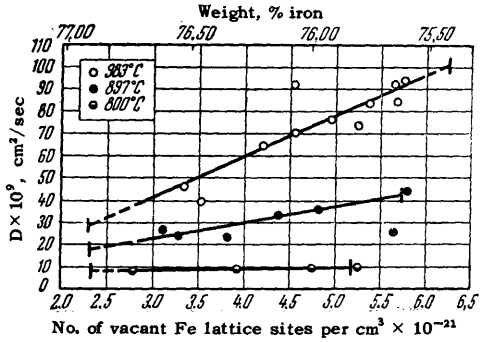

FIG. 18. Self-diffusion coefficient of iron in wüstite as a function of composition. The short vertical bars represent the limits of the wüstite phase field for each temperature. The number of vacant iron lattice sites per unit volume has been calculated from the deviation from stoichiometric composition (77.73%).

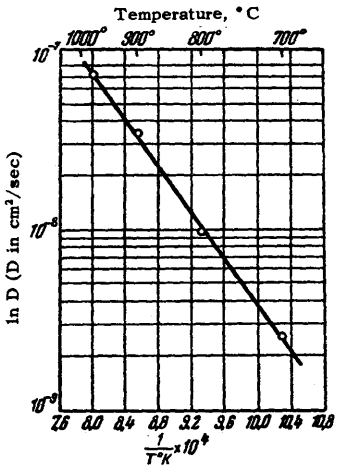

FIG. 19. Temperature dependence of the self-diffusion coefficient of Fe in wüstite for oxides having the composition $Fe_{0.907}O$ (76.02% Fe).

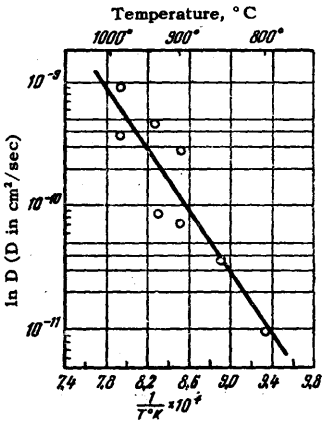

FIG. 20. Temperature dependence of the self-diffusion coefficient of iron in artificial polycrystalline magnetite with average composition $Fe_{2.993}O_4$ (72.38% Fe).

(72.38% Fe) at 750 – 1000° C, $D = 5.2 \exp(-55{,}000/RT)$ (Fig. 20); 3) for hematite α-Fe_2O_3 at 1000° and 1217° C, $D = 4 \times 10^5 \exp(-112{,}000/RT)$ (Fig. 21). The self-diffusion of Fe in hematite was not found to depend on crystallographic direction. The authors compared experimental data on the oxidation rate of iron with theoretical calculations based on Wagner's equation[68] for a system in which the reacting layer is formed directly on the metal surface. Wagner assumed that the migration of iron particles (component 1) is independent of

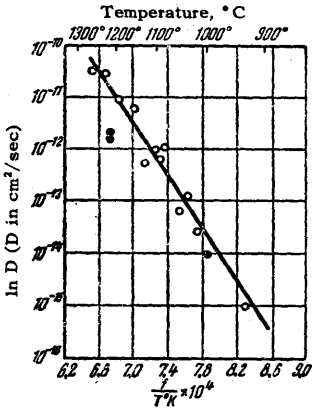

FIG. 21. Temperature dependence of the self-diffusion coefficient of iron in hematite: • – in natural hematite crystals at 1000° and 1217° C; o – in compressed and sintered samples of α – Fe_2O_3, investigated by Lindner.[69]

oxygen migration (component 2), and obtained the following expression for the growth rate of a single oxide on a metal substrate:

$$K_r = |z_2| C_2 \int_{a_2'}^{a_2''} \left(\frac{z_1}{|z_2|} D_1^* + D_2^* \right) d \ln a_2$$

$$= z_1 C_1 \int_{a_1'}^{a_1''} \left(D_1^* + \frac{|z_2|}{z_1} D_2^* \right) d \ln a_1, \ldots \qquad (22)$$

where K_r is the rate constant (or number of chemical equivalents of oxide formed per sec per cm^2 in 1 cm thickness of reaction products), z_1 and z_2 are the valences of iron and oxygen, c_1 and c_2 are the respective concentrations in g-atom/cm^3, a_1 and a_2 are the thermodynamic activities of iron and oxygen in the oxide, and a_1', a_1'', a_2', a_2'' are the limiting values.

Assuming $D_1^* \gg D_2^*$, we can write

$$K_r = |z_2| C_2 \int_{a_2'}^{a_2''} \frac{z_1}{|z_2|} D_1^* d \ln a_2. \qquad (23)$$

The experimental values of K_p given in reference 24 were determined by means of the usual method of weight increase, from

$$\frac{W}{A} = K_p t^{1/2}, \qquad (24)$$

where W is the weight increase (number of grams of added oxygen), A is the surface area of the sample in cm^2, t is time in sec, and K_p is the parabolic rate constant in g-cm^{-2}-$sec^{-1/2}$.

The theoretical equation used for the calculation of K_p was

$$K_{p,\text{calc}}^2 = 16 f_r \rho \alpha K_r, \qquad (25)$$

where f_r is the weight fraction of oxygen in the growing oxide layer, ρ is the density of the oxide layer, and α is a correction for the oxygen transferred from the gas to the oxide. For the growth of wüstite on iron $\alpha = 1$, for that of magnetite on wüstite $\alpha = (1/5 - 1/7)$, and for that of hematite on magnetite $\alpha = 1/9$.

The rate constant K_r calculated on the basis of Wagner's equation, and both the experimental and cal-

culated parabolic growth rates of wüstite, magnetite, and hematite are given in Table III.

The data in the table show satisfactory agreement of experiment and theory for the oxidation of iron. The discrepancy for the growth of hematite on magnetite is attributed by the investigators to the dominant role of oxygen ions and oxide-ion vacancies in the diffusion process, whereas for wüstite and magnetite the dominant diffusion components, in addition to electrons, are iron cations.

On the basis of Wagner's assumption that the transport number for ions is much smaller than that for electrons, τ for iron cations in wüstite can be determined from

$$\sigma\tau = \frac{nz^2e^2D^*}{kT}, \qquad (26)$$

where σ is the electrical conductivity of the oxide, τ is the transport number for the given ion, n is the number of cations per cm^3, z is the valence of the charge carrier, and D is the diffusion coefficient of the charge carrier.

From the self-diffusion and electrical conductivity data, the transport number for Fe^{++} in wüstite was estimated to be 2×10^{-4} at 1000° C.

Our data on diffusion in iron oxides[32,61] were obtained for pressed and sintered samples of Fe_3O_4 (magnetite) at 770 — 1200° C. For the diffusion of iron along grain boundaries $D = 1.27 \times 10^{-3} \times \times \exp(-36{,}200/RT)$; for volume diffusion $D = 0.25 \times \times \exp(-53{,}900/RT)$.

The absorption method yields $D = 9.37 \times 10^{-2} \times \times \exp(-48{,}800/RT)$, which probably represents diffusion along the boundaries and inside of magnetite grains simultaneously.

Lindner used both the contact method and the thin-layer method to investigate Fe diffusion in hematite.[69] Samples made of Fe_2O_3 powder were pressed and sintered at 1200° C. A radioactive layer was applied by hydroxide precipitation from a solution of iron chloride and ammonia, followed by heating at 1000 — 1100° C to produce Fe_2O_3. Fe^{55} was the tracer. For the diffusion of iron in hematite at 750 — 1300° C Lindner obtained $D = 4 \times 10^4 \exp(-112{,}000/RT)$.

Carter and Richardson[27] investigated diffusion in CoO and FeO by means of Co^{60} and Fe^{55}. FeO and CoO disks of 1-mm thickness and 14-mm diameter were prepared by complete oxidation of the metals. FeO was produced at 1000° C in a H_2-water vapor atmosphere; CoO was produced at 1250° C in air.

Sintering and homogenization required 48 hours. The radioactive layer was deposited either chemically, electrochemically, or by vacuum condensation of a radioactive vapor. The adsorption coefficient for FeO is $\mu = 432\ cm^{-1}$. Layers ~3 microns thick were removed by means of carborundum powder. The surfaces of samples were examined microscopically. The following results were obtained: 1) for Fe diffusion in FeO at 700 — 1000° C, $D = 0.014 \exp(-30{,}200/RT)$; 2) for Co diffusion in CoO at 800 — 1350° C, $D = 2.15 \times 10^{-3} \exp(-34{,}500/RT)$.

References 67, 70 and 71 report investigations of Ni diffusion in NiO. It is important to know the diffusion coefficient of nickel cations in NiO in connection with the mechanism that forms this oxide on metallic nickel.

Lindner and Akerström prepared NiO by pressing and sintering the oxide powder at 1100° C.[67] For the diffusion of nickel in nickel oxide at 1140 — 1400° C they obtained $D = 2.8 \times 10^6 \exp(-119{,}500/RT)$, using the short-lived isotope Ni^{65}.

The same investigators subsequently[70] used the long-lived isotope Ni^{63}, obtaining Q = 56,040 ± 1280 cal/mole.

TABLE III. Comparison between the experimental oxide growth (scaling) constants and those calculated from the Wagner equation

Temperature ° C	Calculated rational rate constant, K_r, equivalents/cm-sec	Parabolic scaling constant K_p, $g\text{-}cm^{-2}\text{-}sec^{-1/2}$	
		Theoretical	Experimental
	1. Iron to wüstite		
983	$2.8 \cdot 10^{-8}$	$7.7 \cdot 10^{-4}$	$8.2 \cdot 10^{-4}$
897	$1.1 \cdot 10^{-8}$	$4.8 \cdot 10^{-4}$	$5.0 \cdot 10^{-4}$
800	$0.25 \cdot 10^{-8}$	$2.3 \cdot 10^{-4}$	$2.3 \cdot 10^{-4}$
	2. Wüstite to magnetite		
1100	$9.2 \cdot 10^{-9}$	$1.7 \cdot 10^{-4}$	$1.8 \cdot 10^{-4}$
1050	$4.1 \cdot 10^{-9}$	$1.1 \cdot 10^{-4}$	$1.3 \cdot 10^{-4}$
1000	$1.4 \cdot 10^{-9}$	$0.67 \cdot 10^{-4}$	$0.90 \cdot 10^{-4}$
	3. Magnetite to hematite		
1100	$1.7 \cdot 10^{-12}$	$2.2 \cdot 10^{-6}$	$1.0 \cdot 10^{-4}$
1000	$2.1 \cdot 10^{-14}$	$2.4 \cdot 10^{-7}$	$4.8 \cdot 10^{-5}$

Taik Shim and Moore[71] measured the surface activity of Ni^{63} in order to determine the diffusion of Ni in NiO. Samples of polycrystalline NiO were prepared as follows. Disks of 11-mm diameter were cut out of 0.13-mm nickel foil. These were chemically polished and were then completely oxidized in air at 1250 ± 3° C during 88 hours, after which they were rapidly quenched in nitrogen without acquiring cracks or chips. The disks were then subjected to a homogenizing anneal for 88 hours at 1250° C, followed by a rapid quench. Radioactive Ni^{63} was deposited on monocrystalline NiO plates by means of evaporation from a tantalum wire, on which the isotope had been deposited electrolytically.[72] The activity of the samples was 14,000 counts/min for a 0.044-micron layer. Diffusion annealing was performed in a platinum vessel. Evaporation during this process was not detected when an inactive sample was placed 1 mm above the active sample.

The decrease in surface activity of the tracer is represented in Fig. 22. The diffusion coefficient was obtained from an expression for mixed Ni^{59} and Ni^{63} radiation:

$$\frac{a}{a_0} = \exp(c_1^2 Dt)\,[1 - \operatorname{erf}(c_1^2 Dt)^{1/2}] + \exp(c_2^2 Dt)\,[1 - \operatorname{erf}(c_2^2 Dt)^{1/2}], \quad (27)$$

where c_1, and c_2 are the effective absorption coefficients for Ni^{59} and Ni^{63}, a/a_0 is the activity ratio, and t is time.

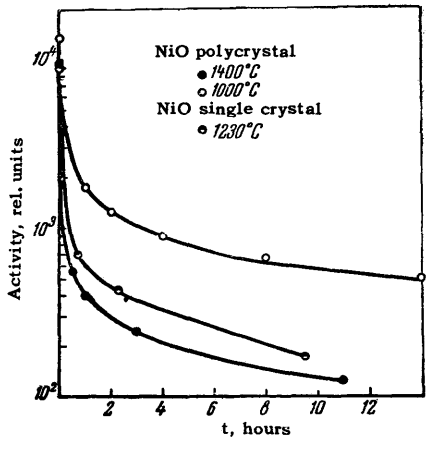

FIG. 22. Decrease of surface activity in NiO after diffusion anneals.

Analysis of the experimental results yields the following values for the self-diffusion coefficients of Ni in nickel oxides: 1) for polycrystalline NiO, $D = 5 \times 10^{-4} \exp(-44{,}200 \pm 600/RT)$; 2) for NiO single crystals, $D = 3.9 \times 10^{-4} \exp(-44{,}200 \pm 200/RT)$. The experimental error in the diffusion activation energy was ~±3 kcal. The oxidation rate constant of nickel, measured at 1 atm pressure of O_2, agrees satisfactorily with diffusion measurements and is represented by $k = 3.8 \times 10^{-4} \exp(-41{,}200/RT)$. The data indicate that the oxidation of Ni under the given conditions results practically entirely from the diffusion of Ni through the NiO lattice, and that diffusion along grain boundaries does not play an important part.

Table II summarizes the data obtained regarding the diffusion of various elements in simple oxides.

2. DIFFUSION IN COMPLEX OXIDES AND REFRACTORIES

The diffusion of radioactive zinc in zinc-iron spinel $ZnOFe_2O_3$ has been studied by Lindner[53] for the purpose of explaining the production of spinel out of the separate solid oxides. $ZnOFe_2O_3$ samples were prepared from equimolar amounts of Zn and Fe precipitated by ammonia. Pellets of 10-mm diameter and 1 — 2 mm thickness, which were hand pressed and sintered in air at 1100° C, had densities between 4.3 and 5.2 g/cm³. The Zn^{65} tracer emits beta and gamma radiation with a 250-day half-life. D was determined by the active thin-layer method and the contact method. In the active thin-layer method the apparatus represented in Fig. 8 was employed. A layer of metallic Zn containing Zn^{65} and weighing 1 mg was deposited by vacuum evaporation on the face of a disk. For the contact method of determining the diffusion coefficient of zinc in ZnO Fe_2O_3 the sample holder together with the sample was inserted into a furnace, as in the case of Zn diffusion in ZnO. The contact method yielded more reliable data than any other technique used here. The exponential dependence of the Zn diffusion coefficient in ZnO Fe_2O_3, as calculated from measurements obtained at 900° to 1350° C for samples annealed in air, has the final form

$$D = 8.8 \cdot 10^2 \exp(-86000/RT).$$

The diffusion of iron in $ZnOFe_2O_3$ was also studied by Lindner,[69] and is of interest in connection with the formation of this spinel through chemical interaction between ZnO and Fe_2O_3. The diffusion coefficient of iron was determined by the contact method and by the expansion, during diffusion, of a thin radioactive layer previously deposited on the surfaces of the samples. The radioactive layer of iron was deposited on $ZnOFe_2O_3$ pellets through hydroxide precipitation from a solution of iron chloride and ammonia, followed by heating at 1000 — 1100° C for one hour to yield Fe_2O_3. The tracer was Fe^{59}. For the diffusion of Fe in $ZnOFe_2O_3$ at 930 — 1270° C the result was $D = 8.5 \times 10^2 \exp(-82{,}000/RT)$. Summarizing, the diffusion coefficient of iron in $ZnOFe_2O_3$ within the investigated temperature range was found to be one order of magnitude higher than for the diffusion of zinc in this spinel, although the activation energy is almost identical for the two cases.

Reference 73 contains data on the diffusion of calcium and iron in calcium monoferrite ($CaOFe_2O_3$). The results are of interest in connection with metallurgical processes (cementation).

Samples of $CaOFe_2O_3$ were prepared by compressing equivalent amounts of CaO and Fe_2O_3 powders to form pellets, which were sintered at 1150 — 1180° C. The tracers were Ca^{45} and Fe^{59}; diffusion annealing was performed in air. The diffusion coefficients of these elements in $CaOFe_2O_3$ were measured by the contact method [employing (2)], and by the expansion of a thin radioactive layer [for Ca^{45}, employing (10)]. In connection with layer grinding the formula used for calculations was

$$D = \frac{x_2^2 - x_1^2}{4t \ln \frac{c_1}{c_2}}, \qquad (28)$$

where t is the diffusion anneal time, x_1 and x_2 are the distances from the original surface of the sample to the boundaries with concentrations c_1 and c_2, respectively. These quantities were obtained from the curve $\ln c = f(x^2)$, which was divided into two straight lines with different slopes corresponding separately to volume diffusion and grain-boundary diffusion in calcium monoferrite. The results for $CaOFe_2O_3$ were as follows: 1) for Fe diffusion at 835 — 1092° C, $D = 3.2 \times \times \exp(-72{,}000/RT)$; 2) for Ca diffusion at 890 — 1140°C, $D = 30 \exp(-86{,}000/RT)$.

In reference 58 Lindner also describes an investigation of Pb^{212} diffusion in $PbOSiO_2$ and $2PbOSiO_2$. Oxides of lead and silicic acids are constituents of many glasses. The samples were sintered compacts of 8 mm diameter and 1.5 mm thickness. For the preparation of a solid metasilicate, analytically pure SiO_2 and PbO were thoroughly mixed and kept in compressed form for one hour at 710° C, after which the pellets were pulverized, repressed, and heated three times for periods of 6 hours at 730° C. Following repulverization the pellets were kept for 1 hour at 745° C, and then at 750° C for 24 hours. The orthosilicate $2PbOSiO_2$ was prepared similarly, with 725° C as the highest sintering temperature.

The density of the metasilicate was 5.2 — 5.5 g/cm³; that of the orthosilicate was 6.8 — 7.0 g/cm³. The diffusion coefficient was determined in four ways, using recoil nuclei, alpha-ray absorption, contact, and layer removal. Pb diffusion at 550 — 700° C in the metasilicate is represented by $D = 8.5 \times 10^{-1} \exp(-59{,}500/RT)$; for the orthosilicate $D = 20 \exp(-47{,}000/RT)$. The diffusion coefficient of Pb in the orthosilicate thus is greater than in the metasilicate; this agrees with the predominance of orthosilicate formation in the reaction between lead oxide and silicic acid.[74] The investigator also noted anomalies in the temperature dependence of D, with the greatest deviation of the metasilicate appearing at 585° C and that of the orthosilicate at 620° C. Figure 23 shows the diffusion anomaly of lead metasilicate. Careful checking led to the suggestion that the anomalies result from changes, such as crack formation, in the diffusion medium.

The methodological interest of this work lies in the division of the diffusion process (Fig. 24) into two processes for lead metasilicate (volume diffusion and grain-boundary diffusion). The linear plot on the left side of the figure represents the concentration as a function of depth in the sample. In the logarithmic plot $c = f(x^2)$ is divided into two straight lines, the first of which ($\ln D = -11.89$) represents concentration close to that obtained by means of the alpha-particle absorption method ($\ln D = -12.0$) and furnishes evidence of volume diffusion, while the second line represents a higher value of the diffusion coefficient ($\ln D = -10.63$), which is characteristic of diffusion along grain boundaries.

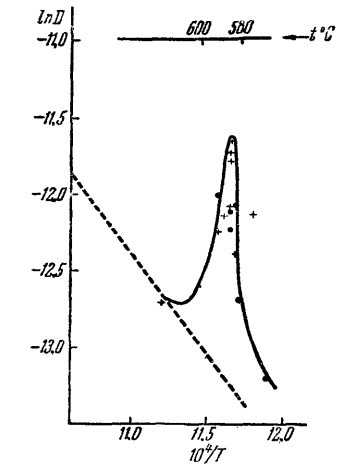

FIG. 23. Diffusion anomaly in lead metasilicate.

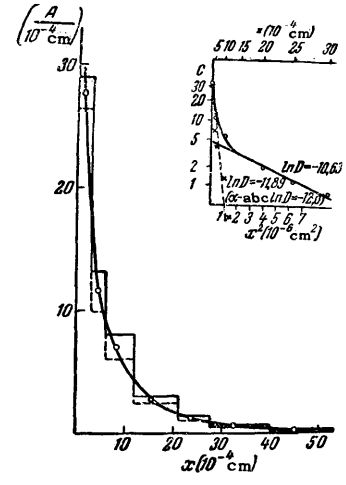

FIG. 24. Pb^{212} concentration in sintered powder compacts of lead metasilicate following diffusion. Both a linear plot and a logarithmic plot (with c given in arbitrary units) are shown.

In reference 26 the "phase-boundary stage" of powder reactions occurring in the formation of calcium and lead silicates was investigated by means of radioactive Ca^{45} and Pb^{212} (ThB). Quartz fractions with grains of sizes 0.04 or 0.06 mm ± 5% were separated by centrifuging. The quartz grains were mixed with a radioactive oxide in 1:2 molar ratio, after which sintered compacts were prepared at suitable temperatures. Following the anneal, the pellets were pulverized for the purpose of removing the unreacted oxide. The activities of two identical weighed samples, following a reaction with silicic acid, were then measured. Figure 3 shows the apparatus used to produce

the red lead oxide. The use of radioactive calcium and lead isotopes permitted determination of the rate constants for the formation of lead and calcium silicates, as follows: for the production of lead silicate at 290 — 380° C ($PbO + SiO_2$), $k = 10^{-7} \exp(-12{,}800/RT)$; for the production of calcium silicate at 1000 — 1300° C ($CaO + SiO_2$), $k = 2.8 \times 10^{-2} \exp(-54{,}000/RT)$ mole-cm^{-2}-sec^{-1}. The parabolic curve for the production of calcium silicate was also used to compute the diffusion coefficients at higher temperatures; these agree approximately with measured values of D for Ca in $CaOSiO_2$.

Later publications (references 28 and 75), which describe reactions in $PbO + SiO_2$ and $CaO + SiO_2$ systems, confirm the results given in reference 58, and also present a detailed analysis of the Wagner mechanism (cation diffusion in the opposite direction through the silicate layer). Si^{31} was used as a tracer in addition to Ca^{45} and Pb^{212} (ThB). It was established qualitatively that silicon does not play an important part in the formation of lead silicates. The short half-life of Si^{31} made it difficult to record measurements. For the diffusion of Ca^{45} in sintered compacts of calcium silicate at 1130 — 1400° C the following results were obtained: for $CaOSiO_2$, $D = 7 \times 10^4 \exp(-112{,}000/RT)$; for $Ca_3Si_2O_7$ below 1260° C, $D = 10^{-2} \exp(-73{,}000/RT)$; for Ca_2SiO_4 with the α-α' transition temperature 1370° C, $D = 3.6 \times 10^{-2} \exp(-65{,}000/RT)$ for α'-Ca_2SiO_4 and $D = 2 \times 10^{-2} \exp(-55{,}000/RT)$ for α-Ca_2SiO_4. It was shown that with increasing strength of the SiO_4 tetrahedral bond the diffusion activation energy for the movement of metal ions is increased. In the case of calcium orthosilicate formation Ca diffusion governs the entire reaction. For the careful investigation of these systems work employing long-lived Si^{32} and O^{18} has been started.

Reference 76 reports an investigation of Ba^{131} self-diffusion in barium metatitanate ($BaOTiO_2$). The half-life of Ba^{131} is 11.7 days. Samples for diffusion experiments were prepared from a powder mixture by means of a reaction between equimolar quantities of analytically pure barium carbonate and titanium oxide at 1365° C. The mixture was twice heated for 10 hours, after which it was pulverized in a mortar. Pellets of 8 mm diameter and 2 mm thickness were prepared. 5% glycerin was added during the compressing process to provide mechanical hardness. The pellets were gradually heated to 1365° C, at which temperature they were maintained for 20 hours; the density was 5 g/cm^3.

D was determined by the contact method and by the expansion of a thin radioactive layer. In the region 884 — 1180° C the plot of $\ln D = f(1/T)$ represents $D_1 = 0.8 \exp(-89{,}000/RT)$. The transport numbers $(1.5 \text{ and } 5) \times 10^{-4}$ and the ion conductivity at 860 — 1135° C give $D_1' = 18 \exp(-58{,}000/RT)$. The accelerated diffusion in the second case is attributed to a change of the material in an electric field.

In reference 63 Linder and Engvist discuss the self-diffusion of tin and zinc in tin-zinc spinel. It is known[77] that the powder reaction between tin oxide and zinc oxide produces the "reverse" spinel $SnZn_2O_4$. For the investigation of Zn and Sn self-diffusion in this spinel, sintered compacts were prepared out of a mixture of ZnO and SnO_2 powders, which were finely pulverized before being pressed. A short sintering period of 15 minutes prevented evaporation of ZnO at 1400 — 1450° C. The density of $SnZn_2O_4$ was 4.2 g/cm^3. Diffusion measurements showed that for Zn in $SnZn_2O_4$ at 1000 — 1250° C, $D = 37 \exp(-76{,}300/RT)$, while for Sn at 1000 — 1260° C we have $D = 2.3 \times 10^5 \times \exp(-109{,}000/RT)$. Calculation of the reaction rate constant for the formation of the spinel (with the dimensions cm^2/sec) led to a curve for $\ln D = f(1/T)$ which was very close to that plotted for Sn diffusion in SnO_2.

Self-diffusion in $NiCr_2O_4$, $ZnCr_2O_4$, $NiAl_2O_4$, and $ZnAl_2O_4$ was measured[67] for the purpose of determining the mechanism involved in the formation of spinels by reactions between solid oxides. Diffusion measurements in these materials are of interest in connection with their formation on alloy surfaces. The spinels were pure oxide compacts whose phase constitution was determined by x rays. Average densities, in g/cm^3, were as follows: $NiCr_2O_4$ — 3.2, $ZnCr_2O_4$ — 3.0, $ZnAl_2O_4$ — 2.2 (in individual instances 3.2), $NiAl_2O_4$ — 2.6. The sintered samples were relatively porous. The sintering temperature reached 1600° C in the case of $NiAl_2O_4$, while for the other spinels it was lower in order to avoid the evaporation of ZnO or Cr_2O_3. In the case of $NiCr_2O_4$, for the diffusion of Ni at 1130 — 1450° C on the basis of eight runs $D = 0.85 \exp(-74{,}600/RT)$, and for the diffusion of Cr on the basis of 10 runs $D = 0.74 \exp(-72{,}500/RT)$; Cr is thus shown to have greater mobility than Ni in this spinel. For $ZnCr_2O_4$ the diffusion of Zn is represented by $D = -60 \exp(-85{,}500/RT)$, while the diffusion of Cr is represented by $D = 8.9 \exp(-81{,}000/RT)$. The results for the diffusion of Zn and Cr in $ZnCr_2O_4$ are provisional because of the limited number of experimental measurements. For Zn in $ZnAl_2O_4$, also on the basis of only a few diffusion runs, we have $D = 2.5 \times 10^2 \exp(-78{,}000/RT)$, while for Ni in $NiAl_2O_4$ we have $D = 3 \times 10^{-4} \exp(-55{,}000/RT)$.

The authors of reference 67 assume that chromite formation is accounted for by Wagner's mechanism, i.e., by cation inter-diffusion, while aluminates are formed by unilateral diffusion (such as that of zinc and oxygen in $ZnAl_2O_4$). The rate constants for exchange reactions between the initial oxides during spinel formation are also compared with diffusion measurements on these processes. The same investigators have published another paper concerning Ni diffusion in nickel spinels.[78]

References 34 and 79 also discuss diffusion in oxides of the spinel type, produced by high-temperature oxidation of Fe-Cr-Al and Ni-Cr-Al alloys contain-

ing small amounts of other elements. The protective properties of the oxides are determined by the strength of their lattice bonds. Cr^{51} and Fe^{59} were used as tracers in these diffusion experiments. Spinels were prepared by compressing oxide mixtures, and a radioactive layer was deposited by vacuum evaporation. The diffusion coefficients and activation energies were found to be in qualitative agreement with the oxidation rates of Ni-Cr and Ni-Cr-Al alloys at high temperatures, and with the evaporation rate of $NiCr_2O_4$. The diffusion experiments were performed in the range 900 — 1200° C. Sun[80] has measured the diffusion of Co and Cr in the chromite spinel $CoCr_2O_4$, which was produced by sintering a mixture of CoO and Cr_2O_3 to form samples with 4.2 g/cm^3 density. Diffusion anneals were performed in air at 1400 — 1600° C. The result obtained for Co diffusion in $CoCr_2O_3$ was $D = 10^{-3} \exp(-51{,}000/RT)$, while for Cr the result was $D = 2 \exp(-70{,}000/RT)$.

The investigation of iron oxide diffusion in refractories[81-83] is important because of the increasingly rigorous specifications for materials used in lining open-hearth and electric steel furnaces. Iron sinter consisting of 55.8% FeO and 42% Fe_2O_3, and containing Fe^{59}, was used as the diffusing material. The samples of refractories were pressed 11×31×20 mm prisms. The original powders were magnesite, chromite, a mixture of 50% magnesite and 50% chromite, and a pulverized heat-resistant industrial magnesite-chromite. The chemical composition is given in the references. Samples were compressed under 1000 kg/cm^2 and were sintered for 2 hours at 1600° C. Diffu-

TABLE IV. Diffusion data for complex oxides

No.	Diffusing substance	Oxide (diffusion medium)	Experimental temperature range, °C	Numerical coefficient of exponential, cm^2/sec	Activation energy, cal/mole	References
1	Zn^{65}	$ZnFe_2O_4$	900—1350	10^3	86000	53
2	Fe^{59}		930—1270	10^3	82000	69
3	Fe	$NiFe_2O_4$	—	$5 \cdot 10^2$	82000	78
4	Fe^{59}	$CaFe_2O_4$	835—1092	3,2	72000	73
	Ca^{45}		890—1140	30	86000	
5	Pb^{212}	$PbOSiO_2$	550—700	$8{,}5 \cdot 10^1$	59500	58
		$2PbOSiO_2$		$2 \cdot 10^1$	47000	
6	Ca^{45}	$CaSiO_3$	1130—1400	$7 \cdot 10^4$	112000	28, 75
		$Ca_3Si_2O_7$	below 1260	10^{-2}	73000	
		α'—Ca_2SiO_4	below the α—α transition, i.e., below 1370	$3{,}6 \cdot 10^{-2}$	65000	
		α—Ca_2SiO_4		$2 \cdot 10^{-2}$	55000	
7	Ba^{131}	$BaOTiO_2$	884—1180	0,8	89000	76
8	Zn^{65}	$SnZn_2O_4$	1000—1250	37	76300	63
	Sn*		1000—1260	$2{,}3 \cdot 10^5$	109000	
9	Ni*	$NiCr_2O_4$	1130—1450	$1{,}5 \cdot 10^{-3}$	61400	67, 78
	Cr^{51}		950—1450	0,75	73000	
10	Cr^{51}	$NiCr_2O_4$	900—1200	$2{,}03 \cdot 10^{-5}$	44800	34, 79
	Fe^{59}			$1{,}35 \cdot 10^{-3}$	61000	
11	Zn^{65}	$ZnCr_2O_4$	1000—1400	60	85000	67, 78
	Cr^{51}			9	81000	
12	Co^{60}	$CoCr_2O_4$	1400—1600	10^{-3}	51000	80
	Cr*			2	70000	
13	Mg	$MgAl_2O_4$	—	$2 \cdot 10^2$	86000	67, 78
14	Zn^{65}	$ZnAl_2O_4$	1000—1400	$2 \cdot 10^2$	78000	
15	Ni^{63}	$NiAl_2O_4$	880—1388	$2{,}9 \cdot 10^{-5}$	53300	34, 79
	Cr^{51}		900—1200	$1{,}17 \cdot 10^{-3}$	50000	
	Fe^{59}			1,33	82000	

sion coefficients for refractories of different compositions were determined by the layer-removal method. With respect to the increase of diffusion rates in the range 1500 — 1700° C the investigated refractories can be arranged in the following order: magnesite, magnesite-chromite, chromite, and Dinas. The authors note that the penetration of iron oxide into refractories is greatly influenced by the chemical interactions between the iron oxides and the constituent phases of the refractories, as well as by the gaseous atmosphere in which the diffusion anneal takes place.

Table IV summarizes the results obtained by different investigators for the diffusion of components in complex metal oxides.

CONCLUSION

The data obtained concerning the diffusion of elements in metal oxides show that the diffusion coefficients of cations in these materials are exponentially temperature-dependent in accordance with Eq. (1). A departure from this law is observed in certain oxides.[58,65] The latter effect is accounted for by changes of the diffusion medium (the appearance of a new phase through chemical transformation during the diffusion anneal of the sample), or by the destruction of the continuity of the oxide (crack formation).

Experiments intended for the measurement of diffusion parameters in oxides involve great difficulties, both in establishing the requisite conditions for avoiding phase changes in the oxides during diffusion anneals, and in setting up the apparatus for such investigations. Data taken from different authors (Tables II and IV) therefore exhibit considerable differences between the coefficients of the exponentials and between the diffusion activation energies obtained for the same systems. The diffusion mechanism involved in the formation of simple oxides or spinel-type compounds is not definitely known. The available data are associated with individually different treatments of the diffusion mechanism in different systems.

It must also be noted how very little quantitative information is available concerning the diffusion of oxygen in oxides. Oxygen migration can be decisive for the chemical reaction involved in the formation of the oxide phase.

Important achievements in the techniques for measuring diffusion coefficients in metals and metal oxides, as well as the directions of further improvements, include devices for continuous recording of radioactive tracer concentration during an entire experimental run and for the control of the oxidizing-reducing medium of furnace gases. Diffusion in metal oxides is sometimes studied in conjunction with kinetic data regarding the growth of oxide layers and phases. Therefore the corresponding data have been compared in some cases.

[1] Z. G. Pinsker, Диффракция электронов (Electron Diffraction), Acad. Sci. Press, Moscow, 1949.

[2] Dankov, Ignatov, and Shishakov, Электронографические исследования окисных и гидроокисных пленок на металлах (Electron-Diffraction Studies of Oxide and Hydroxide Films on Metals), Acad. Sci. Press, Moscow, 1953.

[3] P. D. Dankov, J. Phys. Chem. (U.S.S.R.) **26**, 753 (1952).

[4] O. Kubaschewski and B. E. Hopkins, Oxidation of Metals and Alloys, Academic Press, New York, 1953.

[5] N. S. Gorbunov, Диффузионные покрытия на железе и стали (Diffusion Coating of Iron and Steel), Acad. Sci. Press, Moscow, 1958.

[6] C. Wagner, Diffusion and High Temperature Oxidation of Metals, Atom Movements, Am. Soc. for Metals, Cleveland, 1951.

[7] C. Wagner, Z. physik. Chem. **21**, 25 (1953).

[8] A. M. Zagrubskiĭ, Izv. Akad. Nauk SSSR, Ser. Fiz. **6**, 903 (1937).

[9] J. Groh and G. Hevesy, Ann. Physik **63**, 85 (1920).

[10] J. Groh and G. Hevesy, Ann. Physik **65**, 216 (1921).

[11] W. Frenkel, Z. Physik **35**, 653 (1926).

[12] A. A. Lbov, Usp. Fiz. Nauk **42**, 417 (1950).

[13] R. Lindner, Acta chem. Scand **4**, 307 (1950).

[14] P. L. Gruzin, Doklady Akad. Nauk SSSR **86**, 289 (1952).

[15] B. G. Lyashchenko, Проблемы металловедения и физики металлов (Problems of Metal Research and of the Physics of Metals) Collection 3, Gosmetizd, Moscow, 1952, p. 221.

[16] P. L. Gruzin and D. F. Litvin, Doklady Akad. Nauk SSSR **94**, 41 (1954).

[17] Steigman, Shockley, and Nix, Phys. Rev. **56**, 13 (1939).

[18] A. A. Zhukhovitskiĭ and S. N. Kryukov, Doklady Akad. Nauk SSSR **90**, 379 (1953).

[19] A. A. Zhukhovitskiĭ and V. A. Geodakyan, Doklady Akad. Nauk SSSR **102**, 301 (1955).

[20] Borisov, Golikov, and Lyubov, Izv. Akad. Nauk SSSR, Ser. Tekhn. **10**, 37 (1956).

[21] V. P. Vasil'ev, Doklady Akad. Nauk SSSR **110**, 61 (1956).

[22] Bokshtein, Kishkin, and Moroz, Заводская лаборатория (Factory Laboratory) **3**, 316 (1957).

[23] V. T. Borisov and V. M. Golikov, ibid. **22**, 178 (1956).

[24] Himmel, Mehl, and Birchenall, J. Metals **5**, 827 (1953).

[25] R. Lindner, J. Chem. Soc. (London) Suppl. **2**, 395 (1949).

[26] U. Brune and R. Lindner, Arkiv Kemi **5**, 277 (1953).

[27] R. E. Carter and F. D. Richardson, J. Metals **6**, 1244 (1954).

[28] R. Lindner and E. Spicar, Arkiv Kemi **7**, 565 (1955).

[29] E. A. Socco and W. J. Moore, J. Chem. Phys. **26**, 942 (1957).

[30] R. Lindner, Z. Elektrochem. **54**, 430 (1950).

[31] W. A. Fischer, Silicates industriels **20**, 244 (1955).
[32] V. I. Izvekov, Инж.-физ. журнал (Eng.-Phys. J.) **1**, 64 (1958).
[33] V. I. Izvekov, Приборы и техника эксперимента (Instruments and Exptl. Techniques) **2**, 111 (1957).
[34] Ignatov, Belokurova, and Belyanin, Металлургия и металловедение (Metallurgy and Metal Research) Trans. All-Union Scientific and Technical Conference on the Use of Radioactive and Stable Isotopes and Radiation in the National Economy and in Science, Acad. Sci. Press, Moscow, 1958, p. 326.
[35] O. P. Kramarov and A. M. Seryĭ, Приборы и стенды (Instruments and Test Stands) Inst. Tech. and Econ. Inf., Acad. Sci. USSR, 1956.
[36] V. Jost, J. Chem. Phys. **1**, 466 (1933).
[37] W. Schottky, Z. physik. Chem. **29**, 335 (1935).
[38] R. Lindner and G. Johansson, Acta chem. Scand. **4**, 307 (1950).
[39] Tubandt, Reinhold, and Jost, Z. physik. Chem. **129**, 69 (1927).
[40] Fischbeck and Einecke, Z. anorg. u. allgem. Chem. **177**, 253 (1928).
[41] C. Wagner, Z. physik. Chem. **11**, 139 (1931).
[42] K. E. Zimen, Arkiv Kemi, Mineral. Geol. **A20**, 1 (1945).
[43] S. Flügge and K. E. Zimen, Z. physik. Chem. **42**, 179 (1939).
[44] R. Jagitsch, Ingeniörsvetenskapsakad. handl. **38** (1940); **41** (1941).
[45] F. R. Banks, Phys. Rev. **59**, 376 (1941).
[46] G. de Hevesy and W. Seith, Z. Physik **56**, 790 (1931).
[47] R. Fürth, Handl. physik. techn. Mechanik **7**, 635 (1928).
[48] W. Moore and B. Selikson, J. Chem. Phys. **19**, 1539 (1951).
[49] A. V. Sandulova and A. I. Andrievskiĭ, Doklady Leningrad Polytech. Inst. **2**, No. 1, 23 (1957).
[50] Andrievskiĭ, Karelin, and Sandulova, ibid. **1**, No. 1, 12 (1955).
[51] Andrievskiĭ, Sandulova, and Yurkevich, ibid. **1**, No. 1, 24 (1955).
[52] Andrievskiĭ, Sandulova, and Yurkevich, ibid. **1**, No. 1, 32 (1955).
[53] R. Lindner, Acta chem. Scand. **6**, 457 (1952).
[54] J. P. Roberts and C. Wheeler, Phil. Mag. **2**, 708 (1957).
[55] R. Lindner, Acta chem. Scand. **6**, 468 (1952).
[56] J. P. Blewett, J. Appl. Phys. **10**, 668 (1939).
[57] Zimen, Johansson, and Hillert, J. Chem. Soc., Suppl. **2**, 392 (1949).
[58] R. Lindner, Acta chem. Scand. **5**, 735 (1951).
[59] R. W. Redington, Phys. Rev. **82**, 574 (1951).
[60] N. B. Mikheev, Атомная энергия (Atomic Energy) **6**, 568 (1957).
[61] V. I. Izvekov and K. M. Gorbunova, op. cit. ref. 34, p. 511.
[62] V. I. Izvekov and K. M. Gorbunova, Физика металлов и металловедение (Physics of Metals and Metal Research) **7**, 713 (1959).
[63] R. Lindner and O. Engvist, Arkiv Kemi **9**, 471 (1956).
[64] R. Lindner, Arkiv Kemi **4**, 385 (1952).
[65] R. Lindner and H. N. Terem, Arkiv Kemi **7**, 273 (1954).
[66] H. N. Terem, Compt. rend. **224**, 1351 (1947).
[67] R. Lindner and A. Akerström, Z. physik. Chem. **6**, 162 (1956).
[68] C. Wagner, Z. physik. Chem. **21**, 25 (1933).
[69] R. Lindner, Arkiv Kemi **4**, 381 (1952).
[70] R. Lindner and A. Akerström, Discussions Faraday Soc. **23**, 133 (1957).
[71] Moon Taik Shim and W. J. Moore, J. Chem. Phys. **26**, 802 (1957).
[72] R. Lindner and G. D. Parfitt, J. Chem. Phys. **26**, 182 (1957).
[73] Hedvall, Brisi, and Lindner, Arkiv Kemi **4**, 377 (1952).
[74] R. Jagitsch and B. Bengtsson, Arkiv Kemi Mineral. Geol. **A22**, 1 (1946).
[75] R. Lindner, Z. physik. Chem. **6**, 129 (1956).
[76] A. Garcia-Verduch and R. Lindner, Arkiv Kemi **5**, 313 (1953).
[77] V. Alexandre and A. Garcia-Verduch, Arkiv Kemi **8**, 449 (1956).
[78] R. Lindner and A. Akerström, Z. physik Chem. **18**, 303 (1958).
[79] I. N. Belokurova and D. V. Ignatov, op. cit. ref. 60, **4**, 301 (1958).
[80] R. Sun, J. Chem. Phys. **28**, 290 (1958).
[81] Shvartsman, Pechenov, and Gruzin, Огнеупоры (Refractories) No. 10, 465 (1952).
[82] E. A. Prokof'eva and V. V. Goncharov, op. cit. ref. 34, p. 321.
[83] I. P. Bas'yas, op. cit. ref. 22, **22**, 1437 (1956).

Translated by I. Emin